

Siah Ubiquitin Ligases Modulate Nodal Signaling during Zebrafish Embryonic Development

Nami Kang^{1,3}, Minho Won^{2,3}, Myungchull Rhee^{1,*}, and Hyunju Ro^{1,*}

Siah2 is a zebrafish homologue of mammalian Siah family. Siah acts as an E3 ubiquitin ligase that binds proteins destined for degradation. Extensive homology between *siah* and *Drosophila* Siah homologue (*sina*) suggests their important physiological roles during embryonic development. However, detailed functional studies of Siah in vertebrate development have not been carried out. Here we report that Siah2 specifically augments *nodal* related gene expression in marginal blastomeres at late blastula through early gastrula stages of zebrafish embryos. Siah2 dependent Nodal signaling augmentation is confirmed by cell-based reporter gene assays using 293T cells and 3TP-luciferase reporter plasmid. We also established a molecular hierarchy of Siah as a upstream regulator of FoxH1/Fast1 transcriptional factor in Nodal signaling. Elevated expression of *nodal* related genes by overexpression of Siah2 was enough to override the inhibitory effects of *atv* and *lft2* on the Nodal signaling. In particular, E3 ubiquitin ligase activity of Siah2 is critical to limit the duration and/or magnitude of Nodal signaling. Additionally, since the embryos injected with Siah morpholinos mimicked the *atv* overexpression phenotype at least in part, our data support a model in which Siah is involved in mesendoderm patterning via modulating Nodal signaling.

INTRODUCTION

Siah is the mammalian homologue of the protein encoded by *Drosophila seven in absentia (sina)* that is required for proper R7 photoreceptor development (Carthew and Rubin 1990; Hu et al., 1997; Li et al., 1997; Tang et al., 1997). Various studies showed that both SINA and Siah act as E3 ubiquitin ligase for

target proteins degradation (House et al., 2009; Qi et al., 2013; Wong and Möller, 2013). Since enforced expression of Siah1 causes cellular growth arrest or can be pro-apoptotic (Matsuzawa et al., 1998), Siah proteins were initially reported as tumor suppressors. We also previously reported that transient expression of zebrafish Siah2 in Bosc 23 and HeLa cells induced cell cycle arrest via inhibiting G₂/M phase transition, suggesting that vertebrate Siah family may share their cellular functions (Ro et al., 2003). However, the tumor suppressor function of Siah has been controversial, given the lack of somatic SIAH mutation in human cancers (Medhioub et al., 2000). In addition, several reports support an oncogenic role of Siah proteins in animal cancer model systems (Wong and Möller, 2013)

Vertebrate body patterning is initiated during gastrulation as endoderm, mesoderm and ectoderm are induced along the dorsoventral (DV) and anteroposterior (AP) axes. Fgf, Wnt and Nodal signals initiate early dorsoventral pattern in zebrafish embryos (Schier and Talbot, 2005). After fertilization the dorsal determinants are translocated to the dorsal side through the subcortical microtubules. The dorsal determinants lead to the activation of maternal Wnt signaling. Maternal Wnt, especially Wnt8a in the case of zebrafish activates β -catenin, a transcriptional activator, to regulate expression of several genes important for the early embryonic body patterning (Huelsken and Birchmeier, 2001; Lu et al., 2011). Gore et al. (2005) proposed that Squint (Sqt/Ndr1), one of the Nodal-related proteins, acts as a potent dorsal determinant through the differential localization as early as four cells stage. Previous works showed that Siah1 functions as a negative regulator of the Wnt signaling by down-regulating β -catenin stability (Liu et al., 2001; Matsuzawa and Reed, 2001). Siah2 up-regulates Fgf downstream signaling by destructing Sprouty (a Fgf-dependent ERK inhibitor) in a phosphorylation-independent manner while Siah1 does not (Nadeau et al., 2006; Qi et al., 2008). It thus appears that Siah family plays critical roles in vertebrate body axis formation by modulating various signaling pathways.

Several genetic studies and overexpression experiments indicated that *nodal* related genes are required for the DV and AP patterning (Feldman et al., 1998; Langdon and Mullins, 2011). Nodal belongs to the TGF- β superfamily that transmits signals through heterodimeric type I and type II Activin like receptors (Thisse and Thisse, 1999; Whitman, 2001). Nodal signals lead to formation of a protein complex comprising Smad2/4 and FoxH1 (Fast1; forkhead transcriptional factor) to activate downstream target genes (Attisano et al., 2001; Chen et al., 1997). In zebrafish, two *nodal*-related genes, *squint (sqt/ndr1)*

¹Department of Biological Sciences, College of Bioscience and Biotechnology, Chungnam National University, Daejeon 305-764, Korea, ²Program in Genomics of Differentiation, Eunice Kennedy Shiver National Institute of Child Health and Human Development, National Institutes of Health, Bethesda, Maryland, USA, ³These authors contributed equally to this work.

*Correspondence: mrhee@cnu.ac.kr (MR); rohyunju@cnu.ac.kr (HR)

Received 18 February, 2014; revised 27 March, 2014; accepted 31 March, 2014; published online 14 May, 2014

Keywords: antivin/Lft1, body patterning, FoxH1/Fast1, Nodal, Siah2, zebrafish

and *cyclops* (*cyc/hdr2*) are required for the axial and trunk mesoderm formation as well as endoderm induction (Langdon and Mullins, 2011; Rebagliati et al., 1998). Nodal signaling is also critical for neural patterning, as *sqt;cyc* double mutant or *one-eyed pinhead* (*MZoepe*) mutant embryos lacking an EGF-CFC co-receptor essential for Nodal signaling developed expansion of anterior neural fate and loss of trunk spinal cord (Feldman et al., 1998; Gritsman et al., 1999). Erter et al. (2001) reported that *Wnt8* expression is locally down-regulated at the dorsal midline, but persists ventrolaterally in *sqt;cyc* double mutants or Antivin (*Atv*, a potent nodal antagonist) overexpressed embryos. Since enforced expression of Nodal in the anterior neuroectoderm induces notochord formation at the expense of forebrain (Thisse et al., 2000), it is thus conceivable that Nodal acts as anteriorizing transformer signal for posterior neuroectoderm *via* directly or indirectly up-regulating zygotic *Wnt8* expression in tissues outside of the organizer, specifically the lateral/paraxial mesoderm.

We have previously isolated and characterized a zebrafish Siah and designated it Siaz (renamed to Siah2l following ZFIN designation. But we will call the Siah2l as Siah2 in this report to avoid confusion) (Ro et al., 2003; 2005). In this report, we demonstrated that Siah as a critical intracellular Nodal modulator acts on upstream of Fast1/FoxH1 transcriptional factor for the maintenance of Nodal homeostasis. We revealed that the functional RING domain of Siah2 is exclusively required for antagonizing the function of Nodal inhibitors. Positive roles of Siah for Nodal signaling were reinforced by gene depletion experiments. Knocking-down of Siah1 and Siah2 with specific morpholinos (MO) induced the morphants partially mimicking the morphology of Nodal defective mutants. Collectively, these results clarify the roles of Siah family in Nodal signaling.

MATERIALS AND METHODS

Fish maintenance

Fish and embryos were maintained essentially as described in the zebrafish book (Westerfield, 1995).

Cell culture and transfection

293T cells were grown in Dulbecco's Modified Eagle's medium (DMEM) supplemented 10% fetal bovine serum (FBS). Cells in culture dishes were transfected with various plasmid constructs (pFlag/Siah2, pFlag/Siha2 Mu, pcGlobin2/Siah2, pcGlobin2/Fast-1, pcGlobin2/Fast1-SID) using FuGene6 transfection reagent (Roche). After 24 h, cells were harvested and then the cell pellet was used for further assay.

GST-pull down and Western blotting

In vitro binding assay was performed by mixing embryonic lysates after injecting *GST/β-catenin* or *GST/β-catenin mutant* (stabilized β-catenin) RNA with 10 μl of glutathione-Sepharose 4B (Pharmacia Biotech, Sweden) in total 800 μl volume of NP-40 lysis buffer (150 mM NaCl, 0.02% Na₃, 25 μM PMSF, 1 mM EDTA, 10 mM Tris-Cl, pH 7.2, 0.5% NP-40) at 4°C for 4 h agitation. Precipitates were washed at least three times with ice-cold NP-40 buffer (1 ml) and were analyzed by Western blotting. After separated in SDS-PAGE (10%) and transferred into PVDF membrane, the membrane was incubated for 1 hr under the blocking solution (2% skim milk in PBS with 0.05% Tween-20) at room temperature and then were incubated with anti-Flag (Sigma), anti-β-catenin (Sigma) and anti-GST (Ab Frontier) antibody diluted in blocking solution for 1 h, followed by incubation with HRP-conjugated secondary antibody (Bio-Rad, 1:1000) for 1 h at

room temperature. The detection was performed using Prona™ ECL Ottimo detection system (TransLab).

Luciferase assay

We co-transfected 3TP-Luc reporter construct (0.5 μg) with indicated DNAs into 293T cells using calcium phosphate precipitation technique. Total amount of transfected DNA was equalized with control vectors without inserts. Transfected 293 cells were treated with TGF-β (1 ng/ml) for 24 h, and lysed for luciferase assay using the Dual Luciferase system (Promega).

Whole mount *in situ* hybridization

Antisense riboprobes were constructed using appropriate RNA polymerase following the instructions (Ambion). *In situ* hybridization analysis followed the protocol of Westerfield (1995) with small modification. Proteinase K treatment (10 μg/ml) was performed for 3 to 10 min depending on the stages of embryos. The hybridized probes were detected using pre-absorbed anti-digoxigenin-AP Fab fragments (Roche) diluted (1:2000) in blocking solution (PBS, 0.1% Tween-20, 5% sheep serum). After 3-8 h staining, embryos were mounted in a 2:1 mixture of benzylbenzoate:benzylalcohol and examined under the microscope.

mRNA and MO microinjection

For the microinjection, cDNA constructs were subcloned into the pcGlobin2 vector (Ro et al., 2004b). mRNAs for injection were synthesized from the vector constructs linearized with the appropriate restriction enzymes, using the mMESAGE mMA-CHINE T7 kit (Ambion Inc.) according to the manufacturers instruction. After purification as following the manufacturers recommendation, mRNAs were dissolved in diethylpyrocarbonate (DEPC)-treated 0.1 M KCl. Before injection, the mRNAs were diluted to various concentrations and 1 μl of mRNA was used to inject approximately 400 embryos. The mRNA and MOs were pressure injected into the yolk of 1-2 cell stage of embryos and the injected embryos were raised in 1/3 Ringers solution (39 mM NaCl, 0.97 mM KCl, 1.8 mM CaCl₂, 1.7 mM Hepes, pH 7.2). Injections were performed three to four times to pool the data. To reduce the p53-dependent off-targeting effects of *siah* MOs, we coinjected the MOs with a p63 MO (Robu et al., 2007). MO sequences were: *siah1* translate blocker, 5'-CTGGCGACTCATTCTTCGTCCATA-3'; *siah2* translate blocker, 5'-TCGACGTTTGATGGTGTAAAACCCC-3'.

RT-PCR

Total RNA was isolated from zebrafish embryos using easy-BLUE™ (INTRON, Inc.) and 1 μg of RNA was used for RT-PCR. *sqt* and *β-actin* specific forward and reverse primers were used for this reaction. *sqt*, 5'-CAAGCagaaccgggcaaagacgtcc-3' (forward) and 5'-gtggcagccgattctgcaacaacc-3' (reverse); *β-actin*, 5'-gaggagaccgccgctctgctcac-3' (forward) and 5'-gatggctggaacagggcctctgg-3' (reverse).

Site directed mutagenesis

For the amino acids substitution of Siah2 H107A and C110A, mega-primer was generated by PCR using *Pfu* polymerase (forward primer; 5'-atgagccgtcgctcctctgctgg-3', reverse primer; 5'-gacctgttagccaccagagcccagcctggc-3', Underlines indicate mutated sequences). Generated mega-primer together with another primer (5'-ttagcacatagagatgggtcac-3') was used for the amplification of full length mutated Siah2. Amplified PCR product was subcloned into T-vector (pGEM-T Easy Vector Systems; Promega).

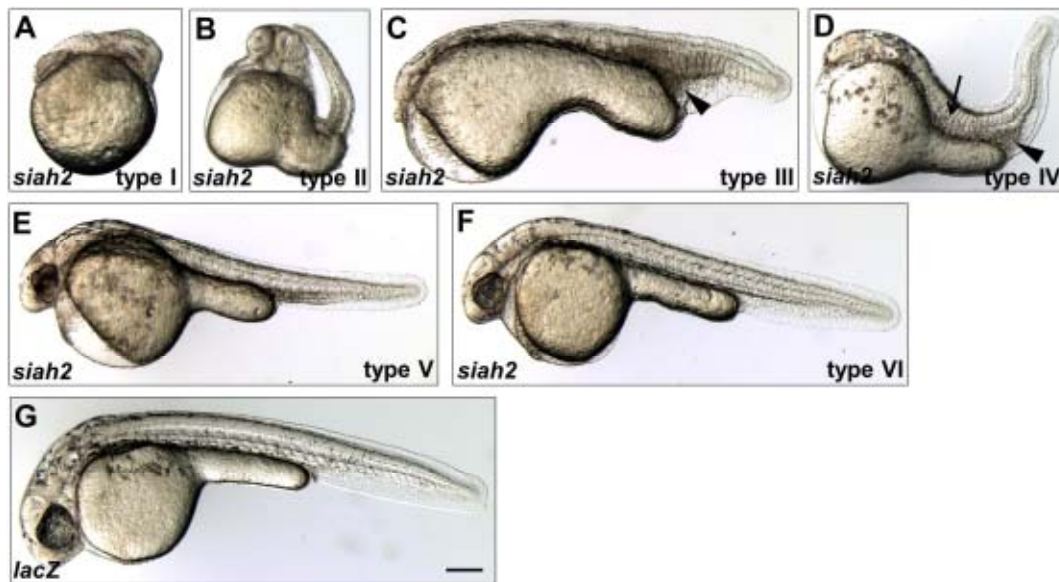


Fig. 1. Injection of *siah2* induces various embryonic defects. Injected embryos were examined using microscopy at 36 hpf (larval view). (A-F) Phenotypes induced by Siah2 overexpression; type I, head rudiments combination with absence of axial structure and trunk; type II, brain defects, degenerated trunk and curled tail structure; type III, extra cells in the tail (arrowhead) and reduced head structure; type IV, partially degenerated notochord (arrow), forebrain defects and extra cell mass in tail (arrowhead); type V, small head and slightly reduced yolk sac; type VI, morphologically indistinguishable from uninjected embryo. (G) Control embryos injected with 500 pg *lacZ* mRNA. Scale bar, 200 μ m.

RESULTS

Siah2 overexpression disturbs early dorso-ventral body pattern

siah2 is maternally expressed and its zygotic expression starts at the mid-blastula transition (MBT) in all blastomeres (Ro et al., 2003). To determine the embryonic function of Siah2, *siah2* RNA (500 pg) was microinjected into the yolk of 1-2 cell stage embryos. When Siah2 was vastly expressed, embryos showed severely dorsalized (Figs. 1A and 1B, $n = 145/305$, 47.5%) or ventralized phenotypes (Figs. 1C and 1D, $n = 63/305$, 21%). Those opposite embryonic defects were reminiscent of the embryos injected with *smad7* RNA (Pogoda and Meyer, 2002). Pogoda and Meyer (2002) showed that overexpression of Smad7 induced phenotypes similar to that of *MZoepr* mutant or *bmp7* mutant (*snh*). The opposite defects caused by Smad7 overexpression might be due to the inhibitory effects of Smad7 on both Nodal and Bmp signaling pathways. To examine if Siah2 modulates two separate signaling pathways for the DV body patterning, we initially analyzed if Siah2 down-regulates β -catenin stability as mammalian Siah1 does (Liu et al., 2001; Matsuzawa and Reed, 2001). β -catenin overexpression caused complete secondary axis formation (Fig. 2A, $n = 54/109$, 49.5%) as well as ectopic expression of *gsc* (Fig. 2C, $n = 41/44$, 93.2%). When Siah2 was co-expressed with β -catenin, the secondary axis formation was nearly abolished (Fig. 2B, $n=19/229$, 8% of embryos formed secondary axis), and ventrolaterally expanded *gsc* expression was suppressed (Fig. 2E, $n = 9/44$, only 20% of embryos showed expanded *gsc* expression). In contrast, N-terminal Ring deleted or C-terminal protein-protein interacting domain deleted form of Siah2 (Ro et al., 2004a) did not suppress the ectopic *gsc* expression (Fig. 2F, $n = 40/44$, 91%; and 2G, $n = 34/39$, 87%, Fig. 2H). Since Siah1 destructs β -catenin independent of GSK-3 (Liu et al., 2001; Matsuzawa and

Reed, 2001), we wondered whether Siah2 destabilizes β -catenin in similar manner. We injected RNA encoding GST-tagged wild type (GST- β -cat) or phosphorylation resistant β -catenin (GST- β -cat Mu) alone or together with *siah2* into 1-2 cell stage embryos, and then detected exogenously supplemented β -catenin using anti- β -catenin antibody or anti-GST antibody after pull-downed using glutathione-sepharose beads. Expression of both WT and phosphorylation resistant β -catenin were remarkably reduced by the co-expression of Siah2 (Figs. 2I and 2J) indicating that Siah2 may induce embryonic ventralization by down-regulating maternally derived Wnt signaling through the destruction of β -catenin.

Interestingly, *squint* (*sqt*) expression increased in the presumptive mesendoderm after *siah2* RNA injection as the expression area expanded from the blastoderm margin toward the animal pole at 40% epiboly (Figs. 3A-3D; embryos with ectopic *sqt* expression: 40% epiboly: 55%, $n = 40$; germ ring: 48%, $n = 44$). *cyclops* (*cyc*) expression was also increased in Siah2 overexpressed embryos (Figs. 3E and 3F; embryos with ectopic *cyc* expression at 40% epiboly: 44%, $n = 45$). The dorsal specific expression domain of *cyc* was largely expanded ventrolaterally in the *siah2* injected embryos (Figs. 3G and 3H; embryos with ectopic *cyc* expression at germ ring: 41%, $n = 41$). These results further support the previous report that dorsalization can be induced by the augmented Nodal signaling (Erter et al., 1998). It is also plausible to consider that the Siah2 dependent embryonic dorsalization, at least to some extent, resulted from dampened zygotic Wnt signaling which is important for the initial specification and maintenance of ventro-posterior mesodermal tissues. Thus, the opposite DV defective phenotypes caused by Siah2 overexpression could be induced by biased diminution of maternal or zygotic Wnt signaling together with elevated induction of *nodal* related genes.

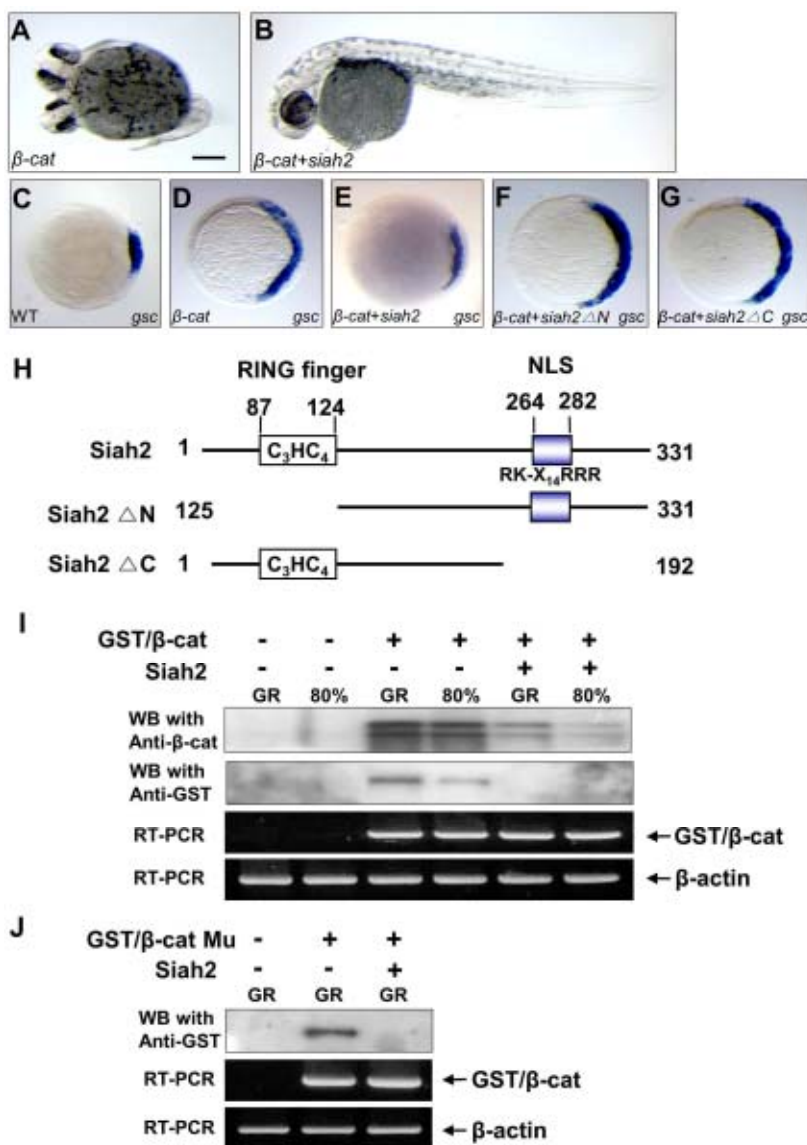


Fig. 2. Siah2 overexpression counteracts β -catenin-induced secondary axis formation via down-regulating β -catenin. Microinjected genes were indicated in the lower left corner of each panel. (A, B) Zebrafish embryos at 36 hpf. (A) WT embryo was injected with 225 pg of β -catenin mRNA. Overexpression of β -catenin induced secondary body axis. (B) Co-injection of β -catenin (225 pg) and *siah2* (100 pg) RNA. Siah2 suppressed hyper-expression of *gsc* by WT or stabilized β -catenin. (C, D) *gsc* expression in the dorsal hypoblast of WT embryos (C) was activated by β -catenin (225 pg) overexpression (D). (E) hyper-expression of *gsc* by β -catenin was suppressed in the embryos co-injected with *siah2* (100 pg). (F, G) N-terminal (Siah2 Δ N) or C-terminal deletion (Siah2 Δ C) of Siah2 failed to suppress hyper-expression of *gsc* by β -catenin. (H) Diagram represents WT and deletion constructs of Siah2. (I, J) Siah2 down-regulates β -catenin in a GSK-3 β -mediated phosphorylation independent manner. GST-pull down of GST- β -catenin with glutathione-Sepharose agarose bead. (I) Embryo extracts from germ ring and 80% epiboly stage injected with GST- β -catenin (225 pg) alone or combination with *siah2* (100 pg). Blots were probed with rabbit polyclonal antibody against β -catenin or anti-GST antibody. (J) Embryo extracts from germ ring and 80% epiboly stage injected with GST- β -catenin Mu (225 pg) alone or together with *siah2* (100 pg). Blots were detected with anti-GST antibody. Note that injected GST- β -catenin or GST- β -catenin Mu mRNAs were not affected by Siah2 overexpression. Ethidium bromide staining of the β -actin RT-PCR products verifies internal control for the reactions. Scale bar, 200 μ m.

Siah2 overexpression restores lefty-induced mesendodermal defects

To ask if the augmented *nodal* related genes expression by Siah2 involves in mesendoderm specification, we co-injected 100 pg of *siah2* RNA with 25 pg of *atv* (*lefty1*) or *lft2* (*lefty2*) RNA. Overexpression of *atv* or *lft2*, the Nodal antagonists, induces severe mesendodermal defects similar to the *MZoe*p or *sqt/cyc* double mutant phenotype (Bisgrove et al., 1999; Schier and Talbot, 2001). *Atv* and *Lft2* compete with Nodal for binding to the type I and II Activin receptor complex (Thisse and Thisse, 1999). As shown in Figs. 4B, 4D, 4Q, and 4S, blocking of Nodal signaling with *atv* or *lft2* overexpression caused severe embryonic defects, such as malformation of embryonic shield, and incomplete mesendoderm-derived tissue formation manifested by fused eyes, no visible notochord and column-like somites in reduced numbers. In contrast, in embryos co-injected with *siah2* RNA development of the embryonic shield, notochord, somites was restored (Figs. 4C, 4E, and 4Q-4T).

We confirmed the antagonizing effects of Siah2 on *Atv/Lft2* by analyzing expression patterns of *shh* and *col2a1*, marker genes for floor plate and notochord, respectively. In the embryos injected with *atv/lft2* RNA (25 pg) alone, the transcripts of both *shh* and *col2a1* were nearly abolished at 24 hpf (Figs. 5A, 5C, 5D, and 5F). But in the embryos co-injected with *atv* (25 pg) and *siah2* RNA (100 pg), expression of *shh* in the floor plate and *col2a1* in the axial mesoderm was restored (Figs. 5G and 5I). The somite defects manifested by severely compromised *myoD* expression in *atv* overexpressed embryos were also rescued by exogenous of Siah2 (Figs. 5B, 5E, and 5H). In addition, the enlarged forebrain at the expense of diencephalon marked with *dlx2* and *emx1* staining in *atv* overexpressing embryos was ameliorated by increased Siah2 expression level (Figs. 5B, 5C, 5E, 5F, 5H, and 5I). We obtained similar results with *lft2* and *siah2* RNA injection (data not shown).

To investigate whether the Siah2 reconstituted *nodal* related gene expression in the developing mesendodermal cells in

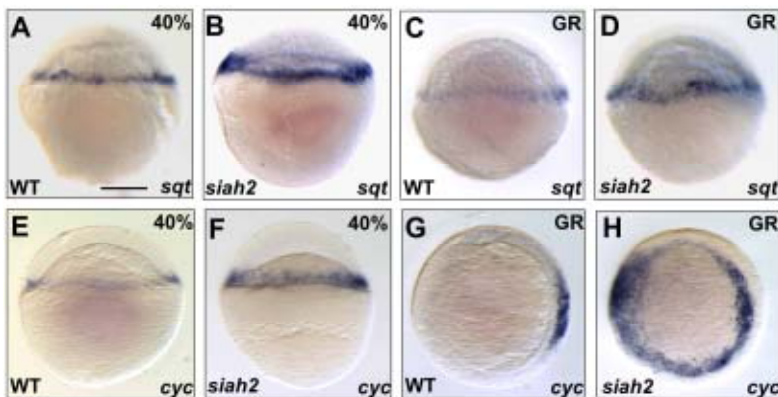


Fig. 3. Siah2 up-regulates *nodal*-related genes. Expression of the marker genes was analyzed by *in situ* hybridization: *sqt* in WT (A, C) and *siah2* injected (B, D) embryos at 40% epiboly (A, B) and germ ring (C, D). *cyc* in WT (E, G) and *siah2* injected (F, H) embryos at 40% epiboly (E, F) and germ ring (G, H). Embryos are shown in the following orientations: lateral view with dorsal to the right (A-F), animal pole view with dorsal to the right (G, H). WT or *siah2* injected embryos are indicated in the lower left corner of each panel; marker genes for expression analysis in the lower right corner of each panel. Scale bar, 200 μ m.

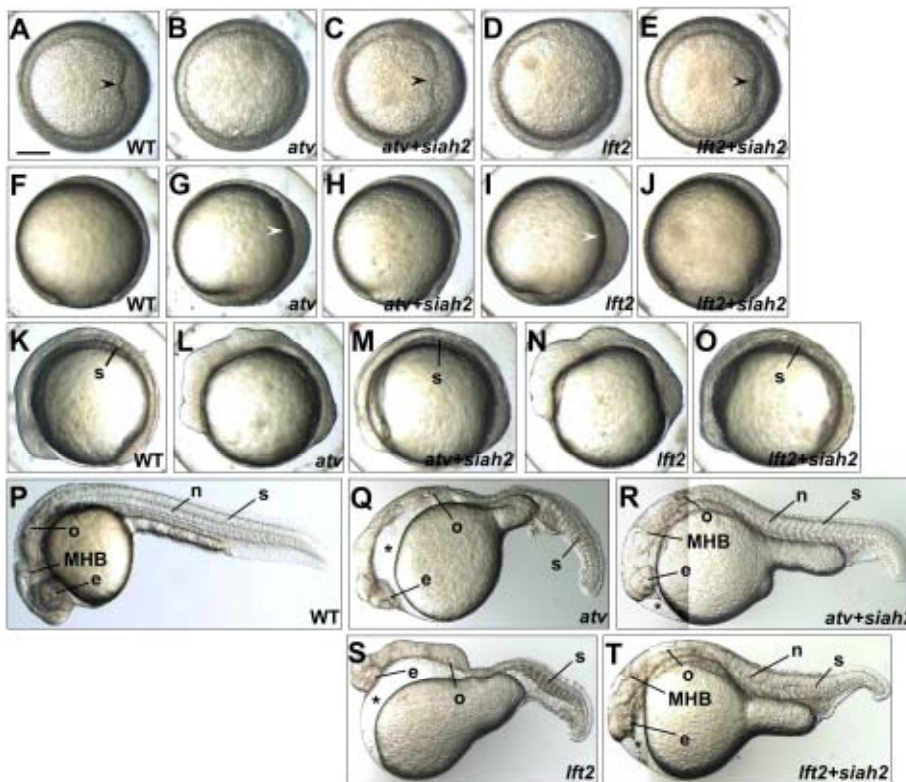


Fig. 4. Siah2 suppresses morphological defects induced by *atv* or *lft2* overexpression. (A, F, K, and P) WT control. Embryonic growth was examined throughout the developmental process. Embryonic shield marked by an arrowhead in (A) was not formed in *atv* (25 pg) or *lft2* (25 pg) injected embryos at 6 hpf (B, D). Shield structure was recovered by *siah2* co-injection (100 pg) (arrowhead, C, E). At 90% epiboly, *atv* or *lft2* injected embryos accumulated cells on the dorsal side (arrowhead, G, I) while *siah2* co-injected embryos did not show the dorsal thickening (H, J). At 5 somites stage, the brain was enlarged and the somites were not visible in *atv* or *lft2* injected embryos (L, N). Co-injected with *siah2* restored the brain and somites structures (M, O). *atv* or *lft2* injection induced cyclopia, lack of anterior mesendoderm, notochord and trunk somites (Q, S). In the absence of notochord, somites with columnar shaped were fused under the neural tube (Q, S). Mesodermal defects were partially restored by *siah2* co-

injection (R, T). Embryos are shown in the following orientations: (A-E) anterior view, dorsal to the right; (F-J) lateral view, dorsal to the right; (K-T) lateral view with anterior to the left. Abbreviations: s, somites; e, eye; o, otic vesicle; n, notochord. Scale bar, 200 μ m.

which the Nodal signaling was experimentally compromised, we injected Nodal antagonist alone or together with *siah2* followed by analyzing *sqt* and *cyc* expression. While *atv/lft2* overexpression abolished *sqt* expression in the marginal blastomeres of late blastula (Figs. 6B and 6D), enforced *siah2* expression overcame the *atv* or *lft2* mediated reduction of *sqt* expression (Figs. 6C and 6E). Additionally, compromised expression of *cyc* was also recovered at least in part by Siah2 (Figs. 6F-6J). The recovery of *nodal* related gene expression by Siah2 was measured further with RT-PCR (Fig. 6K). Taken together, our data suggested that Siah2 stimulates *nodal* re-

lated genes expression in the marginal blastomere at late blastula through early gastrula, and the local stimulation of *sqt* and *cyc* expression in turn overcome inhibitory effects of *atv/lft2*, presumably by overriding competition against Nodal competitive inhibitors.

Fast1/FoxH1 is absolutely required for the Siah2 dependent Nodal augmentation

Because Nodal transduction pathway is mediated by intracellular Smad and FoxH1 (also called Fast1) protein complex (Attisano et al., 2001), we also examined whether Siah2 requires

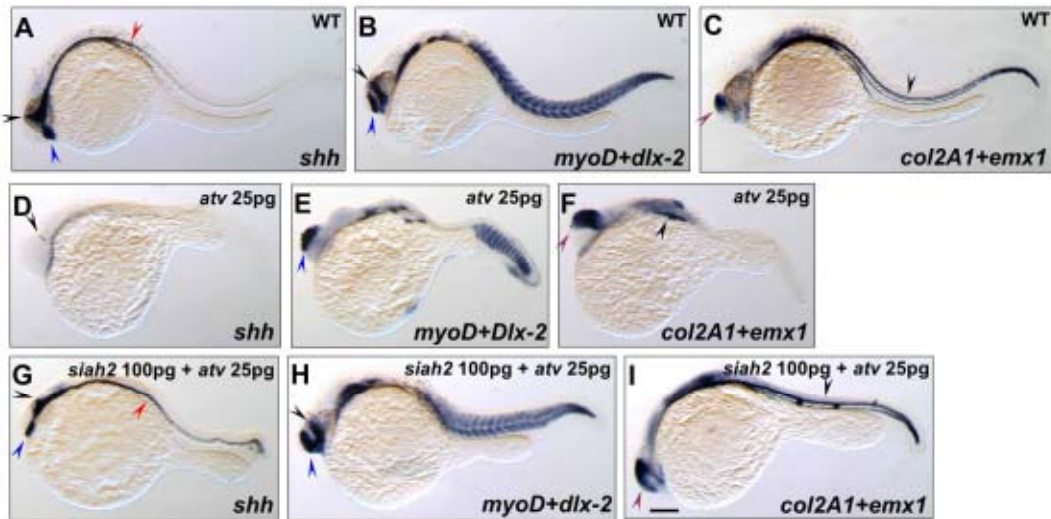


Fig. 5. Siah2 restored the embryonic defects induced by *atv* overexpression. (A, D, and G) Expression of *shh* in the ventral forebrain (blue arrowhead), anterior diencephalon (black arrowhead) and floor plate (red arrowhead) in WT embryos (A), but remarkably reduced in *atv* (25 pg) injected embryo (D), *shh* expression was restored by *siah2* co-expression (G). (B, E, and H) *myoD* expression in the somites (red arrowhead), *dlx2* in the telencephalon (blue arrowhead) and anterior diencephalon (black arrowhead) of WT embryos (B). Pillar like expression of *myoD* was detected in the tail somites of *atv* injected embryos (E). *dlx2* expression in the telencephalon was enlarged at the expense of diencephalon (E). *siah2* co-injection restored wedge like expression pattern of *myoD* in the trunk and *dlx2* expression in the brain (H). (C, F, and I) Expression of *col2A1* in the notochord (red arrowhead) and *emx1* in the telecephalon (blue arrowhead) of a control embryo (C). Absence of notochord and enlarged telencephalon was obvious in *atv* injected embryos (F). Siah2 overexpression rescued notochord and forebrain defects (I). All embryos were fixed at 24 hpf. Lateral view, anterior to the left. Scale bar, 200 μ m.

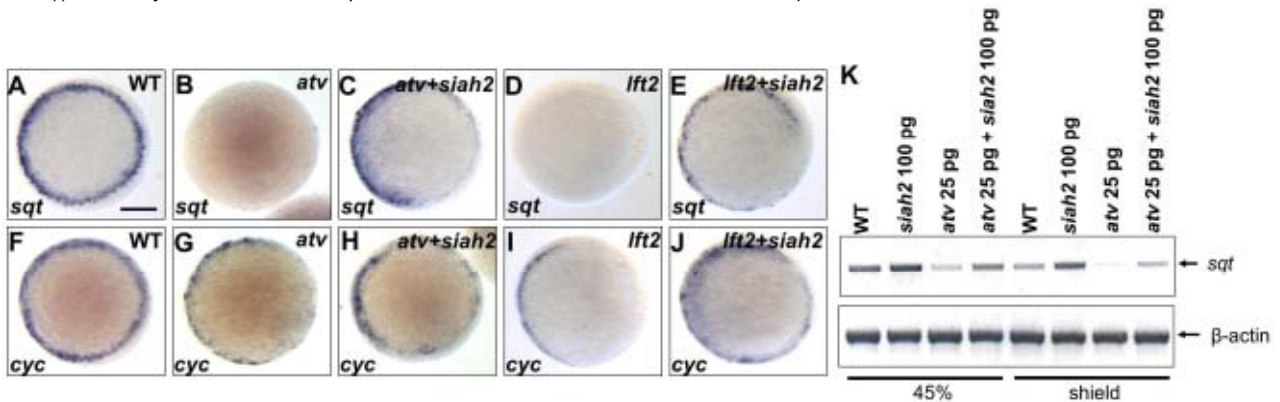


Fig. 6. Siah2 antagonizes the *Atv* or *Lft2* activity. *sqt* (A-E) and *cyc* (F-J) transcripts were detected by *in situ* hybridization. (A) *sqt* expression was detected in the marginal blastomere of uninjected embryo at 45% epiboly stage. (B, D) *sqt* transcription was completely suppressed in *atv* or *lft2* RNA injected embryos. (C, E) *siah2* co-injection restored the expression of *sqt* in the blastoderm margin. (F) *cyc* transcripts appeared in the marginal blastomeres of uninjected embryo at 45% epiboly. (G, I) *atv* or *lft2* RNA injection suppressed *cyc* expression from dorsal to the ventro-lateral margin. (H, J) Siah2 restored the *cyc* expression in the marginal blastomeres. (K) RT-PCR analysis with injected embryos at 45% epiboly and embryonic shield stage. Embryos were injected with RNA encoding *siah2* (100 pg) and/or *atv* (25 pg). PCR (27 cycles) was carried out with primers as "Materials and Methods". β -actin PCR products were loaded as a loading control. (A-J) Animal pole view, dorsal to the right side. Scale bar, 200 μ m.

the intracellular elements for its biological functions. We initially analyzed the effects of WT and dominant negative form of Fast1 on *sqt* transcripts. Embryos were injected with dominant negative *fast1* (only containing Smad binding domain; *fast1-SID*; 0.5 ng) (Pogoda et al., 2000) alone or together with *siah2* (*Fast1-SID*; 0.5 ng + *siah2*, 0.1 ng). Overexpression of *fast1-SID* markedly reduced *sqt* transcripts in the marginal blastomere (9/20 lost, 10/20 showed reduced expression of *sqt*; Figs. 7A and 7B) and developed the phenotype of *MZsur*, a maternal

and zygotic mutant encoding two point mutations in forkhead domain of FoxH1 (data not shown) (Sirotkin et al., 2000). Embryos injected with *fast1-SID* and *siah2* showed decreased or eliminated *sqt* expression in the blastoderm margin as well (10/22 lost, 10/22 reduced expression of *sqt*; Fig. 7C). However, Siah2 enhanced 3TP (containing 3 copy of Smad binding element of PIA1 gene)-Luc reporter gene activity (Fig. 7D) upon TGF- β stimulation while Fast1-SID suppressed the reporter gene stimulated by Siah2 with TGF- β treatment (Fig. 7D).

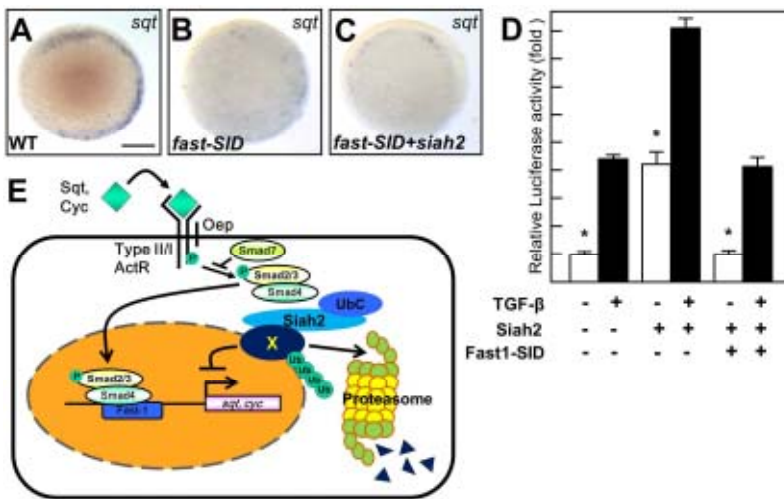


Fig. 7. Ectopic Nodal induction by Siah2 is FoxH1/Fast1 dependent. (A) *sqt* expression in wild type. (B) *fast1-SID* injection suppressed *sqt* expression. (C) *siah2* co-injection with *fast1-SID* failed to induce *sqt* expression. (D) Measurement of luciferase activity. p3TP-Luc reporter plasmid was co-transfected with pcGlobin 2/Siah2 and/or pcGlobin 2/Fast1-SID (Dominant negative Fast1) in the presence or absence of TGF-β stimuli. While Siah2 enhanced the expression of PIA1 gene-driven luciferase reporter (3TP-Luc) with dosage dependent manner, Fast1-SID suppressed the reporter activity driven by Siah2. (E) A model illustrating Siah2 dependent Nodal signaling augmentation. Considering our results and previous reports, we proposed a model that ligands, such as Sqt and Cyc, bind to type II activin like receptor with an aid of EGF-

CFC/Oep co-receptor, which in turn activates type I activin like receptor. The activated type I receptor phosphorylates Smad2, and then the phosphorylated Smad2 binds with Smad4. The Smad2/4 translocates into nucleus to form a large transcriptional protein complex with Fast-1. The transcriptional complex re-activates *nodal* related genes through a positive feedback loop. We postulate that Siah2 (presumably together with Siah1) targets unidentified protein X which might serve as an intracellular Nodal signaling inhibitor for proteasome dependent protein degradation. *significance was taken as $P < 0.05$ Student's *t*-test. Scale bar, 200 μm.

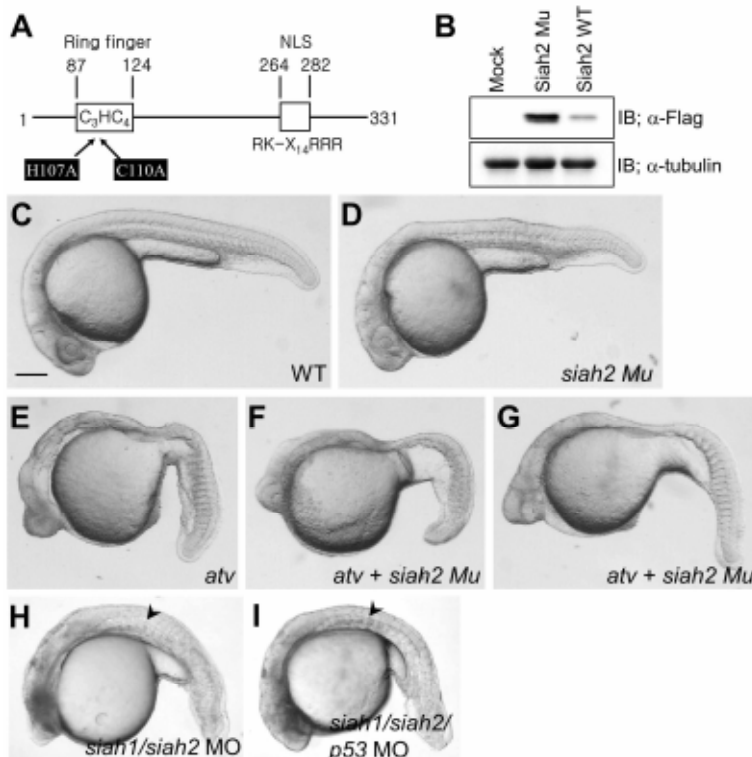


Fig. 8. E3 ubiquitin ligase activity of Siah2 is critical for antagonizing Antivin function. (A) Diagram represents RING mutated amino acid residues of Siah2. (B) Flag-tagged WT *siah2* or RING mutated Siah2 (*siah2 Mu*) were transfected into 293T cell. Anti-Flag antibody was used to detect transfected WT Siah2 or Siah2 Mu (Top). The same membrane (middle) was stripped and blotted with α-tubulin as a loading control (bottom). (C) WT embryo. (D) 200 pg *siah2 Mu* RNA injected embryo. (E) 25 pg *atv* RNA injected embryo. (F) 25 pg *atv* RNA was co-injected with 200 pg *siah2 Mu* RNA. (C-F) All live embryos were taken picture at 24 hpf. Lateral view, anterior to the left. Arrowheads in (H) and (I) indicate notochord. Scale bar, 200 μm.

These studies suggest that Siah2 requires Fast1 transcription factor to stimulate transcription of Nodal downstream genes, such as *nodal* related genes themselves. Because the Siah2 dependent 3TP-Luc reporter gene activity was additive to TGF-β stimuli (Fig. 7D), we propose that Siah2 may exert its biological function in TGF-β independent manner. It is thus conceivable that TGF-β and Siah2 mediated gene induction pathways

merge into Fast1/FoxH1, and that Siah2 may destabilize unidentified intracellular TGF-β/Nodal inhibitor(s) by exploiting ubiquitin proteasome system (UPS) (Fig. 7E).

E3 ubiquitin ligase activity of Siah2 is required for Nodal signaling

Siah proteins bind E2 ubiquitin conjugating enzymes via N-

terminal RING domain and interact with proteins targeted for degradation *via* C-terminal domain (Wong and Möller, 2013). Given that *nodal* related gene expression was augmented by Siah2 overexpression, we introduced two point mutations into the C₃HC₄ zinc RING finger domain by substituting core histidine and cysteine residues with alanine (H107A, C110A) (Siah Mu) to eliminate Siah2 E3 ubiquitin ligase activity (Fig. 8A). Flag tagged WT *siah2* or *siah Mu* were transfected into the 293T mammalian cells, of which the cellular extracts were subject to immunoblotting. As shown in Fig. 8B, the increased stability of Siah2 by inducing mutations indicated that E3 ubiquitin ligase activity was inactivated in Siah Mu. Embryos overexpressing Siah Mu developed overall WT-like morphology with certain degree of cell growth retardation and shortened body size (Fig. 8D). When Siah Mu was co-expressed with Antivin, Siah Mu was unable to rescue the phenotypic defects induced by Nodal blockage (Figs. 8E-8G). These results clearly argue that E3 ubiquitin ligase activity of Siah2 is essential for transducing proper Nodal signaling.

Siah depleted embryos partly mimics Nodal defective phenotype

To explore the *in vivo* function of Siah during early embryonic development, we depleted both Siah1 and Siah2 using antisense morpholinos (MO). As shown in Figs. 8H and 8I, Siah depleted embryos exhibited severe body defects with shorten axis and defected mesodermal tissues somewhat similar to the embryos with compromised Nodal signaling. It is noteworthy that since the only tissue necrosis presumably due to *siah* MO toxicity was significantly ameliorated by inhibiting p53 function without any improved body structure of the morphants, we concluded that the embryonic defects induced by depletion of Siah1 and Siah2 were not simply due to the MO toxicity but mainly due to the compromised Siah function during early embryonic development. However, a rudimentary notochord was still observed in *siah* morphants, and the columnar shape of somites, which is the another hallmark of Nodal deficiency, was less obvious in *siah* morphants. In addition, contrary to our expectations, *siah* morphants showed equivalent expression of *sqt* and *cyc* at 40% epiboly to WT (data not shown). There are at least two possible explanations for the unexpected results. First, the maternally deposited Siah deviated from MO targeting might compensate the early induction of mesendodermal cells in zebrafish embryos. Second, the Siah might be less permissive but more instructive to the Nodal signaling during early embryonic development, even if compound Siah1a and Siah2 mutant mice showed neonatal lethality without any overt histological defects (Frew et al., 2003). Therefore, generation of Siah1a, Siah1b and Siah2 triple compound mutant mice will be necessary to identify whether the Siah dependent Nodal signaling is conserved across species. Nevertheless, the defective mesendoderm derived tissues in the *siah* morphants argues that Nodal signaling is positively influenced by endogenously expressed Siah.

DISCUSSION

Highly conserved Siah homologues have been identified in fly, mouse, zebrafish and human. Here we reported that Siah augmented a sufficient quantity of *nodal related genes* expression in the marginal blastomeres, which is enough to override the competition against the biological functions of Nodal antagonists (Atv and Lft). Given the reported E3 ubiquitin ligase activities of Siah family and the versatile physiological function

of UPS system (Anuppalle et al., 2013; Qi et al., 2013), it is worth consideration that Siah may target intracellular inhibitor(s) of Nodal signaling for proteasome dependent protein destruction to increase the duration or magnitude of the expression of *nodal* related genes. Although several Siah target proteins involved in diverse cellular signaling pathways have been identified (House et al., 2009), there are lack of any *in vivo* evidences for the physiological function of Siah in TGF- β or Nodal signaling pathway.

One of the plausible targets of Siah in Nodal signaling is TIEG1, a transcriptional repressor of *smad7* promoter, which can be targeted for destruction by Siah (Jonhson et al., 2002). Thus, TIEG1 enhances TGF- β /Smad signaling by inhibiting negative feedback regulation loop mediated by inhibitory Smad7 (Johnsen et al., 2002). Given when Smad7 was overexpressed in zebrafish, the embryos showed dorsalized or ventralized, sometimes both combined phenotype due to the binary inhibition of Nodal and BMP signaling by Smad7 (Pogoda and Meyer, 2002), which is reminiscent of the embryos with elevated Siah2 expression by mRNA injection (Fig. 1). In this context, we tested if Siah2 stimulates *smad7* expression in the marginal blastomeres by down regulating TIEG1 protein stability. However, *siah1* or *siah2* mRNA injection failed to expand *smad7* expression level during early to mid-gastrula stage (data not shown). This observation may be explained by the fact that, in the absence of growth factor, TIEG1 is scarcely expressed at levels which could not show any biological activity (Johnsen et al., 2002). Thus, we concluded that TIEG1 may not be the major target of Siah for the maintenance of proper Nodal signaling, even if we cannot exclude the possibility that the relatively low cellular level of TIEG1 regulated by Siah somewhat contributes to the maintenance of Nodal homeostasis.

Another putative target of Siah in Nodal signaling is Zic2. Houston and Wylie (2005) showed that maternally supplied *Zic2* suppressed the expression of several *Xenopus* nodal related (*Xnr*) genes in early development. Depletion of maternally expressed *Zic2* in *Xenopus* embryos resulted in exogastrulation, anterior truncation and axial defect. In addition, loss of maternal *Zic2* caused increased expression of *Xnr* genes, and hyper-activation of Nodal signaling. However, we failed to detect physical association between Siah2 and Zic2 (data not shown). Since Zic2 was not poly-ubiquitylated and not destabilized by Siah, we ruled out Zic2 as a target molecule of Siah.

Iratni et al. (2002) reported that transcriptional corepressor DRAP1 interacts with Fast-1 and inhibits DNA binding. Interestingly, the DRAP1-deficient mice showed expanded *Nodal* expression in primitive streak, while the *lft2* transcription was largely diminished in nascent mesoderm (Iratni et al., 2002). Therefore, DRAP1 was one of the attractive candidates of Siah. However, DRAP1 does not contain well conserved Siah degron sequence (RPVAXVxPxxR; VxP is the core Siah binding motif) (House et al., 2003; Möller et al., 2009) across the species and may not physically interact with Siah2.

We previously identified a novel Siah2 interacting partner designated as Sinup using yeast two-hybrid screening with Siah2 as bait (Ro et al., 2005). Overexpression of *sinup* induced *cyclopa*-like phenotype, reminiscent of the *Zeop* mutant, but did not affect the mRNA level of *sqt* and *cyc* (Ro et al., 2005). Thus, we concluded that the fused-eye phenotype induced by Sinup overexpression was not due to the attenuated Nodal signaling by the elevated level of Sinup, but simply due to the anterior neural plate defects.

A previous report showed that T84 epithelial cells treated with TGF- β down regulates Siah1 and Siah2 expression level when

the cells were cultured three-dimensionally (Juuti-Uusitalo et al., 2006). Recently, Liao et al. (2012) also reported that undifferentiated small intestinal crypt cells (IEC-6 cell line) in response to TGF- β stimuli increased the expression of miRNA-146b, which induced *SIAH2* mRNA decay presumably through direct interaction between the seed region of miRNA-146b and its complementary sequences of *SIAH2* 3'UTR. Although it is not clear whether the TGF- β dependent Siah regulatory loop is generic feedback mechanism, the previous reports (Juuti-Uusitalo et al., 2006; Liao et al., 2012) suggested that *nodal* related gene expression can be negatively regulated by Nodal itself through suppressing Siah expression, which rendered the further complexity of the regulatory loop of Nodal signaling. However, at least in zebrafish, since the Siah1 and Siah2 are largely accumulated as maternal transcripts, the maternally deposited *siah* transcripts may contribute the onset as well as maintenance of *nodal* related genes expression during late blastula and early gastrula stage. Collectively to our knowledge, this is the first report unveiling hidden utility and function of Siah on the way to augment *nodal* related genes expression for the maintenance of Nodal homeostasis. Obviously, identification of target proteins of Siah in Nodal signaling will extend our understanding molecular paradigm governing vertebrate embryogenesis.

ACKNOWLEDGMENTS

We thank I.B. Dawid (NIH-NICHD, USA) for the valuable comments for and thorough reading of our manuscript. This research was supported by Basic Science Research Program through the National Research Foundation of Korea (NRF) funded by the Ministry of Education, Science and Technology (NRF-2012R1A1A4A01012264).

REFERENCES

- Anuppalle, M., Maddirevula, S., Huh, T.R., and Rhee, M. (2013). Ubiquitin proteasome system networks in the neurological disorder. *Anim. Cells Syst.* *17*, 383-387.
- Attisano, L., Silvestri, C., Izzi, L., and Labbe, E. (2001). The transcriptional role of Smads and FAST (FoxH1) in TGF- β and activin signalling. *Mol. Cell. Endocrinol.* *180*, 3-11.
- Bisgrove, B.W., Essner, J.J., and Yost, H.J. (1999). Regulation of midline development by antagonism of lefty and nodal signaling. *Development* *236*, 3253-3262.
- Carthew, R.W., and Rubin, G.M. (1990). *seven in absentia*, a gene required for specification of R7 cell fate in the *Drosophila* eye. *Cell* *63*, 561-577.
- Chen, X., Weisberg, E., Fridmacher, V., Watanabe, M., Naco, G., and Whitman, M. (1997). Smad4 and FAST-1 in the assembly of activin-responsive factor. *389*, 85-89.
- Erter, C.E., Solnica-Krezel, L., and Wright, C.V. (1998). Zebrafish nodal-related 2 encodes an early mesendodermal inducer signaling from the extraembryonic yolk syncytial layer. *Dev. Biol.* *204*, 361-372.
- Erter, C.E., Wilm, T.P., Basler, N., Wright, C.V., and Solnica-Krezel, L. (2001). Wnt8 is required in lateral mesendodermal precursors for neural posteriorization *in vivo*. *Development* *128*, 3571-3583.
- Feldman, B., Gates, M.A., Egan, E.S., Dougan, S.T., Rennebeck, G., Sirotkin, H.I., Schier, A.F., and Talbot, W.S. (1998). Zebrafish organizer development and germ-layer formation require nodal-related signals. *Nature* *395*, 181-185.
- Frew, I.J., Hammond, V.E., Dickins, R.A., Quinn, J.M., Walkley, C.R., Sims, N.A., Schnall, R., Della, N.G., Holloway, A.J., Digby, M.R., et al. (2003). Generation and analysis of Siah2 mutant mice. *Mol. Cell. Biol.* *23*, 9150-9161.
- Gore, A.V., Maegawa, A., Cheong, A., Gilligan, P.C., Weinberg, E.S., and Sampath, K. (2005). The zebrafish dorsal axis is apparent at the four-cell stage. *Nature* *438*, 1030-1035.
- Gritsman, K., Zhang, J., Cheng, S., Heckscher, E., Talbot, W.S., and Schier, A.F. (1999). The EGF-CFC protein one-eyed pinhead is essential for nodal signaling. *Cell* *97*, 121-132.
- House, C.M., Frew, I.J., Huang, H.L., Wiche, G., Traficante, N., Nice, E., Catimel, B., and Bowtell, D.D. (2003). A binding motif for Siah ubiquitin ligase. *Proc. Natl. Acad. Sci. USA* *100*, 3101-3106.
- House, C.M., Möller, A., and Bowtell, D.L. (2009). Siah protein: novel drug targets in the ras and hypoxia pathways. *Cancer Res.* *69*, 8835-8838.
- Houston, D.W., and Wylie, C. (2005). Maternal Xenopus Zic2 negatively regulates Nodal-related gene expression during antero-posterior patterning. *Development* *132*, 4845-4855.
- Hu, G., Chung, Y.L., Glover, T., Valentine, V., Look, A.T., and Fearon, E.R. (1997). Characterization of human homologs of the *Drosophila* seven in absentia (*sina*) gene. *Genomics* *46*, 103-111.
- Huelsken, J., and Birchmeier, W. (2001). New aspects of Wnt signaling pathways in higher vertebrates. *Curr. Opin. Genet. Dev.* *11*, 547-553.
- Iratni, R., Yan, Y.T., Chen, C., Ding, J., Zhang, Y., Price, S.M., Reinberg, D., and Shen, M.M. (2002). Inhibition of excess nodal signaling during mouse gastrulation by the transcriptional corepressor DRAP1. *Science* *298*, 1996-1999.
- Johnsen, S.A., Subramaniam, M., Monroe, D.G., Janknecht, R., and Spelsberg, T.C. (2002). Modulation of transforming growth factor (TGF- β)/Smad transcriptional responses through targeted degradation of TGF- β -inducible early gene-1 by human seven in absentia homologue. *J. Biol. Chem.* *277*, 30754-30759.
- Juuti-Uusitalo, K.M., Kaukinen, K., Mäki, M., Tuimala, J., and Kainulainen, H. (2006). Gene expression in TGFbeta-induced epithelial cell differentiation in a three-dimensional intestinal epithelial cell differentiation model. *BMC Genomics* *7*, 279.
- Langdon, Y.G., and Mullins, M.C. (2011). Maternal and zygotic control of zebrafish dorsoventral axial patterning. *Annu. Rev. Genet.* *45*, 357-377.
- Li, S., Li, Y., Carthew, R.W., and Lai, Z.C. (1997). Photoreceptor cell differentiation requires regulated proteolysis of the transcriptional repressor tramtrack. *Cell* *90*, 469-478.
- Liao, Y., Zhang, M., and Lönnerdal, B. (2012). Growth factor TGF- β induces intestinal epithelial cell (IEC-6) differentiation: miR-146b as a regulatory component in the negative feedback loop. *Genes Nutr.* *8*, 69-78.
- Liu, J., Stevens, J., Rote, C.A., Yost, H.J., Hu, Y., Neufeld, K.L., White, R.L., and Matsunami, N. (2001). Siah-1 mediates a novel β -catenin degradation pathway linking p53 to the adenomatous polyposis coli protein. *Mol. Cell* *7*, 927-936.
- Lu, F.I., Thisse, C., and Thisse, B. (2011). Identification and mechanism of regulation of the zebrafish dorsal determinant. *Proc. Natl. Acad. Sci. USA* *108*, 15876-15880.
- Matsuzawa, S., and Reed, J.C. (2001). Siah-1, SIP, and Ebi collaborate in a novel pathway for β -catenin degradation linked to p53 responses. *Mol. Cell* *7*, 915-926.
- Matsuzawa, S., Takayama, S., Froesch, B.A., Zapata, J.M., and Reed, J.C. (1998). p53-inducible human homologue of *Drosophila* seven in absentia (Siah) inhibits cell growth: suppression by BAG-1. *EMBO J.* *17*, 2736-2747.
- Medhioub, M., Vaury, C., Hamelin, R., and Thomas, G. (2000). Lack of somatic mutation in the coding sequence of SIAH1 in tumors hemizygous for this candidate tumor suppressor gene. *Int. J. Cancer* *87*, 794-797.
- Möller, A., House, C.M., Wong, C.S., Scanlon, D.B., Liu, M.C., Ronai, Z., and Bowtell, D.D. (2009). Inhibition of Siah ubiquitin ligase function. *Oncogene* *28*, 289-296.
- Nadeau, R.J., Toher, J.L., Yang, X., Kovalenko, D., and Friesel, R. (2006). Regulation of Sprout2 stability by mammalian Sevenin-Absentia homolog 2. *J. Cell Biochem.* *100*, 151-160.
- Pogoda, H.M., and Meyer, D. (2002). Zebrafish Smad7 is regulated by Smad3 and BMP signals. *Dev. Dyn.* *224*, 334-349.
- Pogoda, H.M., Solnica-Krezel, L., Driever, W., and Meyer, D. (2000). The zebrafish forkhead transcription factor FoxH1/Fast1 is a modulator of nodal signaling required for organizer formation. *Curr. Biol.* *10*, 1041-1049.
- Qi, J., Nakayama, K., Gaitonde, S., Goydos, J.S., Krajewski, S., Eroshkin, A., Bar-Sagi, D., Bowtell, D., and Ronai, Z. (2008). The ubiquitin ligase Siah2 regulates tumorigenesis and metastasis by HIF-dependent and -independent pathways. *Proc. Natl. Acad. Sci. USA* *105*, 16713-16718.
- Qi, J., Kim, H., Scortegagna, M., and Ronai, Z.A. (2013). Regulators and effectors of Siah ubiquitin ligases. *Cell Biochem. Bio-*

- phys. 67, 15-24.
- Rebagliati, M.R., Toyama, R., Haffter, P., and Dawid, I.B. (1998). cyclops encodes a nodal-related factor involved in midline signaling. *Proc. Natl. Acad. Sci. USA* 95, 9932-9937.
- Ro, H., Kim, K.E., Huh, T.L., Lee, S.-K., and Rhee, M. (2003). Expression pattern of Siaz gene during the zebrafish embryonic development. *Gene Exp. Patterns* 3, 483-488.
- Ro, H., Jang, Y., and Rhee, M. (2004a). The ring domain of Siaz, the zebrafish homologue of *Drosophila* seven in absentia, is essential for cellular growth arrest. *Mol. Cells* 17, 160-165.
- Ro, H., Soun, K., Kim, E.-J., and Rhee, M. (2004b). Novel vector systems optimized for injecting *in vitro*-synthesized mRNA into zebrafish embryos. *Mol. Cells* 17, 373-376.
- Ro, H., Won, M., Lee, S.U., Kim, K.E., Huh, H.L., Kim, C.H., and Rhee, M. (2005). Sinup, a novel Siaz-interacting nuclear protein, modulates neural plate formation in the zebrafish embryos. *Biochem. Biophys. Res. Commun.* 332, 993-1003.
- Robu, M.E., Larson, J.D., Nasevicius, A., Beiraghi, S., Brenner, C., Farber, S.A., and Ekker, S.C. (2007). p53 activation by knock-down technologies. *PLoS Genet.* 3, e78.
- Schier, A.F., and Talbot, W.S. (2001). Nodal signaling and the zebrafish organizer. *Int. J. Dev. Biol.* 45, 289-297.
- Schier, A.F., and Talbot, W.S. (2005). Molecular genetics of axis formation in zebrafish. *Annu. Rev. Genet.* 39, 561-613.
- Sirotkin, H.I., Gates, M.A., Kelly, P.D., Schier, A.F., and Talbot, W.S. (2000). Fast1 is required for the development of dorsal axial structures in zebrafish. *Curr. Biol.* 10, 1051-1054.
- Tang, A.H., Neufeld, T.P., Kwan, E., and Rubin, G.M. (1997). PHYL acts to down-regulate TTK88, a transcriptional repressor of neuronal cell fates, by a SINA-dependent mechanism. *Cell* 90, 459-467.
- Thisse, C., and Thisse, B. (1999). Activin, a novel and divergent member of the TGF- β superfamily, negatively regulates mesoderm induction. *Development* 126, 229-240.
- Thisse, B., Wright, C.V., and Thisse, C. (2000). Activin- and Nodal-related factors control antero-posterior patterning of the zebrafish embryo. *Nature* 403, 425-428.
- Westerfield, M. (1995). *The Zebrafish book: a guide for the laboratory use of zebrafish (Danio rerio)* (University of Oregon Press).
- Whitman, M. (2001). Nodal signaling in early vertebrate embryos: themes and variations. *Dev. Cell* 1, 605-617.
- Wong, C.S., and Möller, A. (2013). Siah: a promising anticancer target. *Cancer Res.* 73, 2400-2406.